ISSN 0020-4412, Instruments and Experimental Techniques, 2018, Vol. 61, No. 1, pp. 99–105. © Pleiades Publishing, Ltd., 2018.

GENERAL EXPERIMENTAL TECHNIQUES

Single Camera 3D Digital Image Correlation Using a Polarized System[1]

Junrui Li[a], Boyang Zhang[a], Xin Kang[a, b], Wan Xu[a], Guobiao Yang[a], and Lianxiang Yang[a, *]

[a] *Department of Mechanical Engineering, School of Engineering and Computer Science, Oakland University, Rochester, USA*

[b] *Department of Mechanical Engineering, School of Mechanical and Electrical Engineering, Putian University, Putian, China*

**e-mail: yang2@oakland.edu*

Received February 16, 2017

Abstract— In this paper, a novel single camera three dimensional digital image correlation (3D-DIC) system, using a polarized pseudo-stereo system, is proposed. Compared to traditional 3D-DIC systems using stereo-vision, it has a more compact structure and better vibration resistance. Compared to the conventional single camera pseudo-stereo system that splits the CCD sensor into two halves to capture the stereo views, the proposed system achieves both views using the entire CCD chip without reduction of the spatial resolution. In addition, the center of the two views stands in the center of the CCD chip, similarly to conventional 3D-DIC systems, thus minimizing the image distortion compared to the conventional pseudo-stereo system. The two overlapped views in the CCD sensor are separated using the different polarization states, and the standard 3D-DIC algorithm can be utilized directly to perform the evaluation. The principal and experimental setup are described in detail, and multiple tests are performed to validate the system.

DOI: 10.1134/S0020441218010050

1. INTRODUCTION

Digital image correlation (DIC) is a non-contact, whole-field optical measurement method capable of measuring the contour, deformation and strain on a surface. This technique was proposed by Peters, [1], Sutton [2], and Yamaguchi, [3] in the 1980s. Starting in the mid-1990s, the three-dimensional digital image correlation (3D-DIC) technique was developed to obtain whole-field information, including the contour, deformation, and strain, in three dimensions [4].

In the 3D-DIC technique, the conventional DIC algorithm is integrated with a stereo-vision system to fulfill the 3D measurement. Two fixed cameras with an angle between them were placed in front of the test object, and the stereo-vision algorithm was applied to combine the information from these two cameras [5, 6]. In addtion, to determine the intrinsic and extrinsic parameters for the stereo-vision system, the 3D calibration technique for the DIC system was investigated at the same time [7–9].

Several problems currently exist in the 3D-DIC system. First, the conventional 3D-DIC system is sensitive to environmental vibration [10, 11]. Since the conventional 3D-DIC system uses two cameras to acquire the 3D information, the relative position between the cameras must be fixed to obtain accurate results after calibration. The environmental vibration could result in relative movement between the cameras, thus introducing error to the measurement. Second, the conventional 3D-DIC system has limitations with respect to high speed measurement. 3D-DIC requires that two images be captured at the same time for 3D measurement. However, this requires precise synchronization between the two high speed cameras, and the synchronization between the camera could change over the course of the measurement. Lastly, the conventional 3D-DIC has the difficulties with measuring small areas [12]. Through extension of the applications of 3D-DIC, 3D-DIC has been used for material testing within a small area. A long focus lens needs to be utilized to obtain good image resolution. However, the long focus lens is usually large in size, which results in a position conflict between the two lenses in the conventional system.

To overcome the drawbacks of the conventional 3D-DIC system, K. Genovese proposed a single camera 3D-DIC setup utilizing the refraction-based pseudo-stereo system in 2013 [13]. A bi-prism, as a refractor, is used to split the scene into two equivalent lateral views in the two halves of the CCD chip. The single camera 3D-DIC system acheives the 3D-DIC

[1]The article is published in the original.

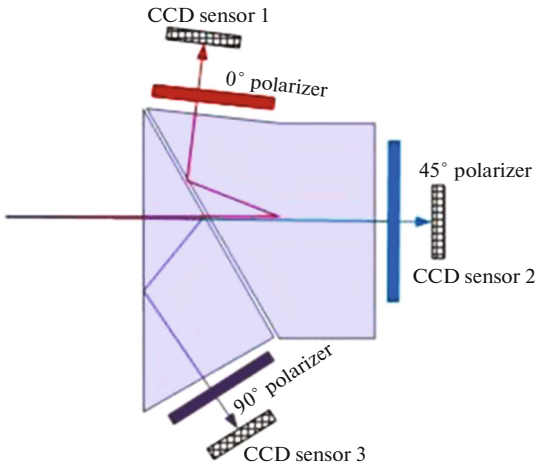

Fig. 1. Schematic view of polarization camera.

measurement with a single camera, and provides a new path for achieving 3D-DIC [14–16].

However, two problems still exist in the proposed single camera 3D-DIC system. First, image distortion occurs due to the utilization of the refractor and the lateral offset of the scene. Second, the resolution of each view reduces in half due to splitting the scene. To solve these drawbacks, a new dimension needs to be utilized to separate the two views instead of splitting the scene in the CCD chip.

Digital image correlation, as a mathematical algorithm, is only sensitive to the intensity of light, making it possible to use the other properties of light to separate the views. The wavelength and polarization state are two common properties which can be utilized to separate two lights with different optical paths. Bandpass color filters and color cameras can be combined to fulfill the image separation with different wavelength 17. However, loss of light of the bandpass filter could be a serious issue with this method.

The light can be easily polarized with the polarizer; however, a single camera has to be able to capture polarized light with different angles to fulfill this technique. Recently, the polarization camera has been investigated and developed to capture polarized images. These type of cameras have been widely used in medical, machine vision and defense applications [18–20]. The schematic view of the polarization camera is shown in Fig. 1.

In this paper, a single camera 3D-DIC system using a polarized pseudo-stereo system is proposed. Two filters with a perpendicular polarized angle are combined with the reflection-based pseudo-stereo system to filter the two views from the different optical paths. Two images with different polarization states can be captured by a single polarization camera. The two views are captured in different signal channels separated by the different polarization states. With this single camera 3D-DIC system, both views use the whole CCD chip, and no spatial resolution reduction occurs. The principles and experimental setup are introduced in detail in the following sections. An experimental validation is performed, and the results obtained by the proposed system are compared with a commercial 3D-DIC system.

2. PRINCIPAL AND THE THEORY OF THE SYSTEM

The scheme of the proposed system is shown in Fig. 2. A reflection-based pseudo-stereo system is utilized to obtain the two views from the different perspectives. Two mirrors reflect the two images with different perspectives to the beamsplitter. The two views are then combined within the beamsplitter and cap-

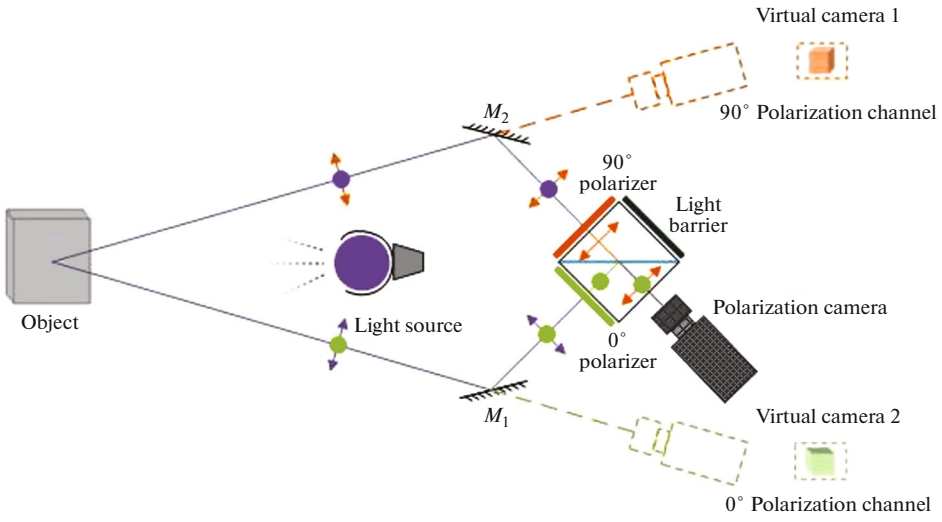

Fig. 2. Scheme of the single camera 3D-DIC using a polarized pseudo-stereo system.

Table 1. Measured displacement in *y* direction by two systems at same location

Step no.	Polarized system, mm	Standard system, mm	Error, mm
0	0	0	0
1	−0.196954	−0.18397	0.012984
2	−0.362529	−0.357763	0.004766
3	−0.558495	−0.561468	0.002973
4	−0.736176	−0.748647	0.012471
5	−0.941347	−0.950341	0.008994
6	−1.04603	−1.05011	0.00408

tured by the polarization camera. Two polarizers with perpendicular polarization angles (0° and 90°) are placed in front of the beamsplitter to prevent mixing of the views. The two lights are polarized with different polarization angles after passing the polarizers. The dots and arrows in this figure represent the direction of the polarization. Two images with different polarization angles are separated in the polarization camera.

The principle of the single camera 3D-DIC system using a polarized pseudo-stereo system is very similar to the conventional stereo-vision 3D-DIC system. The difference between the two systems is that two virtual cameras, as shown in Fig. 2, replace the two physical cameras in the conventional system. The scheme of the coordinate systems is shown in Fig. 3. The transformation from image coordinate (2D coordinate, obtained from the polarized image) to virtual camera coordinate (3D coordinate) using the pinhole camera model is displayed below:

$$\alpha^i \mathbf{x}^i_{\text{image}} = \mathbf{P}^i \times \mathbf{x}^i_{\text{vc}},$$

$$\mathbf{P} = \begin{bmatrix} f & 0 & 0 & 0 \\ 0 & f & 0 & 0 \\ 0 & 0 & 1 & 0 \end{bmatrix}, \quad \mathbf{x}^i_{\text{image}} = \begin{bmatrix} x^i_{\text{image}} \\ y^i_{\text{image}} \\ 1 \end{bmatrix}, \quad \mathbf{x}^i_c = \begin{bmatrix} x^i_{\text{vc}} \\ y^i_{\text{vc}} \\ z^i_{\text{vc}} \\ 1 \end{bmatrix}, \tag{1}$$

where **P** is the projection matrix which projects the 3D coordinate to a 2D plane; f is the focus of the lens of the single camera; α^i is the scale factor; $\mathbf{x}^i_{\text{image}}$ and $\mathbf{x}^i_{\text{vc}}$ is the image coordinate and virtual camera coordinate of the ith virtual camera, respectively.

The pseudo-stereo system requires that the two virtual camera coordinates be merged to a single world system. In addition, the distortion due to the imaging system needs to be corrected. The transformation between the ith virtual camera coordinate to the world coordinate is expressed as:

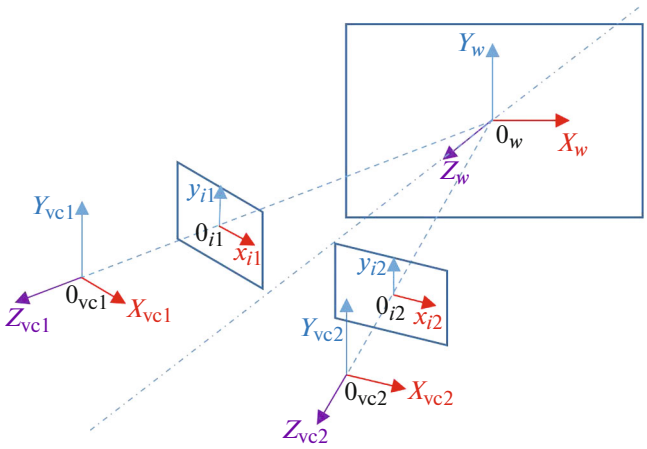

Fig. 3. Scheme of the coordinate systems of the pseudo-stereo 3D-DIC.

$$\mathbf{x}^i_{\text{vc}} = \mathbf{T}^i \times \mathbf{x}_w,$$

$$\mathbf{T}^i = \begin{bmatrix} \mathbf{r}^i & \mathbf{t}^i \\ 0 & 1 \end{bmatrix}, \quad \mathbf{D}^i \times \mathbf{A}^i \times \mathbf{P}^i \times \mathbf{x}^i_{\text{vc}} = \alpha^i \mathbf{x}^i_{\text{image}}, \tag{2}$$

$$\mathbf{r}^i = \begin{bmatrix} r^i_{11} & r^i_{12} & r^i_{13} \\ r^i_{21} & r^i_{22} & r^i_{23} \\ r^i_{31} & r^i_{32} & r^i_{33} \end{bmatrix}, \quad \mathbf{t}^i = \begin{bmatrix} t^i_x \\ t^i_y \\ t^i_z \end{bmatrix},$$

where $\mathbf{T}^i$ represents the transformation matrix which transforms the camera coordinate of the virtual camera to the world coordinate of the pseudo-stereo system, and $\mathbf{r}^i$ and t^i are the rotational component and translational component, respectively. $\mathbf{D}^i$ and $\mathbf{A}^i$ is the distortion and skew adjust matrix, which can be determined using different distortion or skew models. $\mathbf{x}_w$ is the world coordinate of the pseudo-stereo system.

The single camera 3D-DIC system must be calibrated to determine all these intrinsic and extrinsic parameters. Since the principal of the pseudo-stereo system is quite similar to the conventional 3D-DIC system, the classical calibration procedure of the conventional 3D-DIC system can be utilized directly. The direct linear transform (DLT), as a standard calibration method for the stereo-vision system, is widely used for calibration in conventional 3D-DIC. The transformation equation to determine the system parameters using the DLT method is expressed as [17]:

$$\begin{cases} u^i - u^i_0 = f\alpha^i_u \dfrac{(r^i_{11}x + r^i_{12}y + r^i_{13}z + t^i_x)}{(r^i_{31}x + r^i_{32}y + r^i_{33}z + t^i_z)}, \\ v^i - v^i_0 = f\alpha^i_v \dfrac{(r^i_{21}x + r^i_{22}y + r^i_{23}z + t^i_y)}{(r^i_{31}x + r^i_{32}y + r^i_{33}z + t^i_z)}. \end{cases} \tag{3}$$

In the above equation, u^i and v^i are the image coordinates of the ith virtual camera in the horizontal and

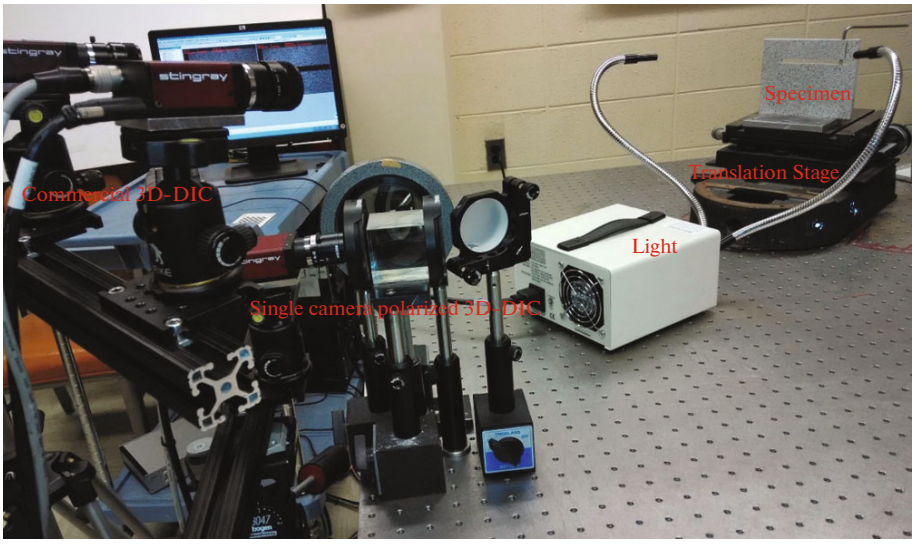

Fig. 4. Experimental setup of the validation test.

vertical direction, respectively; u_0^i and v_0^i are the coordinate at the center point in the horizontal and vertical direction, respectively; f is the focus of the lens; and α_u^i and α_v^i are the scale factors in the horizontal and vertical direction, respectively. Components r^i and t^i are components of the transformation matrix $\mathbf{T}^i$.

Finally, the two images obtained by the different channels of the polarization camera can be evaluated using the DIC algorithm. Since the image from the right optical path is only reflected once, the image of this view has to be digitally flipped horizontally to obtain the correct view for the DIC evaluation.

3. EXPERIMENTAL TESTS AND THE RESULT

To validate the proposed system, a set of experimental tests were performed. An industrial camera with an adjustable polarizer was used to simulate the polarization camera, as a polarization camera was not available for use. The image with the 0°/90° polarization angle, which can directly be obtained from the polarization camera, now is obtained by successively rotating the polarizer.

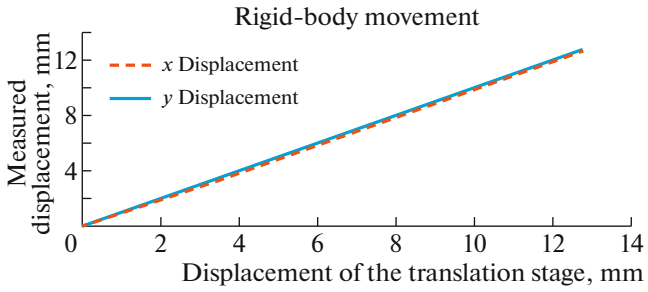

Fig. 5. Displacement under a rigid-body movement.

Two types of tests were performed to validate the system. The first test performed was a rigid-body movement test. This test was performed to validate the accuracy of the displacement measurement. The second test performed was a strain measurement test. For this test, the strain measurement results were compared with the results from a commercial conventional 3D-DIC system.

3.1. Displacement Measurement

A notched aluminum alloy plate was used as the test sample in this experiment. The specimen was 10 mm thick and fixed at the bottom. The notch was created on the upper part of the plate. The plate was fixed on a two dimensional (2D) linear translation stage, making it easy to produce an accurate in-plane (x-direction) and out-of-plane (z-direction) displacement. Additionally, a micrometer screw was installed at the end of the cantilevered part to introduce a compression loading to the specimen. The displacement in the y direction that was produced by the compression was measured by both the polarized single camera 3D-DIC system and a commercial 3D-DIC system. The results obtained from the commercial system were regarded to be the true value.

The experimental setup is shown in Fig. 4. For this test, the specimen was moved in both the in-plane (x-direction) and out-of-plane (z-direction) from 0 to 12.7 mm with 2.54 mm intervals. The average rigid-body movement over the surface, shown in Fig. 5, shows good consistency in the movement direction.

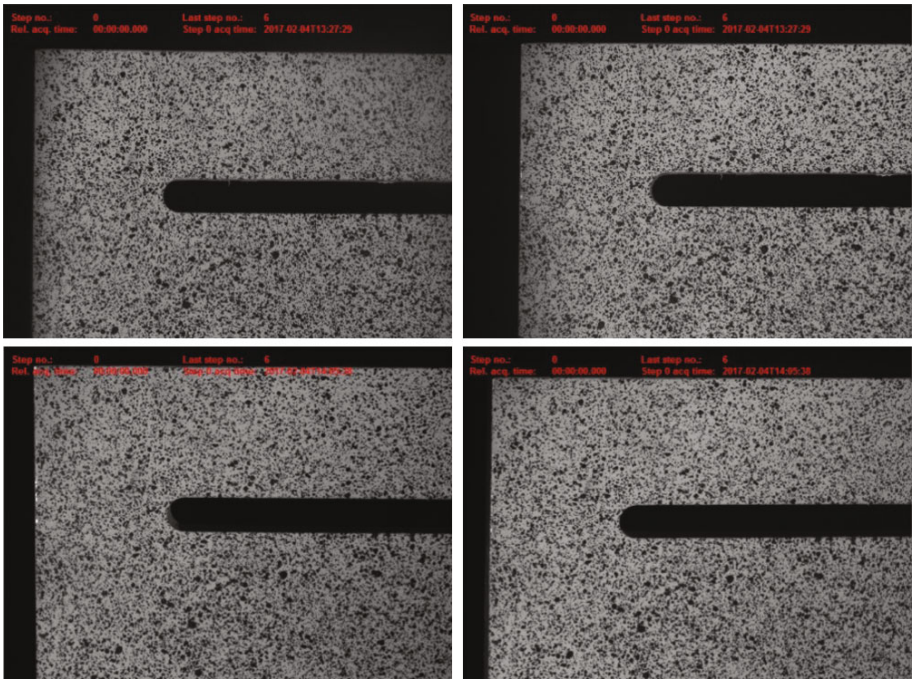

Fig. 6. Raw images captured by the two systems: upper, proposed system, lower, standard system.

To further study the accuracy of the displacement measurement, the displacement in the y direction of the cantilever part, resulting from the compression produced by the screw, is measured by the polarized single camera 3D-DIC system and a commercial 3D-DIC system. The raw images captured by the two systems are shown in Fig. 6, and the measurement results are displayed in Fig. 7. Table shows the displacement in the y direction at the position of the cantilever shown in Fig. 7. As shown in Table 1, the maximum measurement error of the proposed system is around 0.01 mm.

3.2. Strain Measurement

A mild steel sheet metal specimen was used for the strain measurement test. Two notches were created at the center of the specimen to produce a strain concentration during deformation. A bending moment was applied to the sheet metal to produce bending at the center of the specimen. The strain produced by the bending was measured by the polarized single camera 3D-DIC and the commercial 3D-DIC simultaneously. The raw images of the specimen before and after deformation is shown in Fig. 8. The strain distribution resulting from image evaluation is shown in Fig. 9.

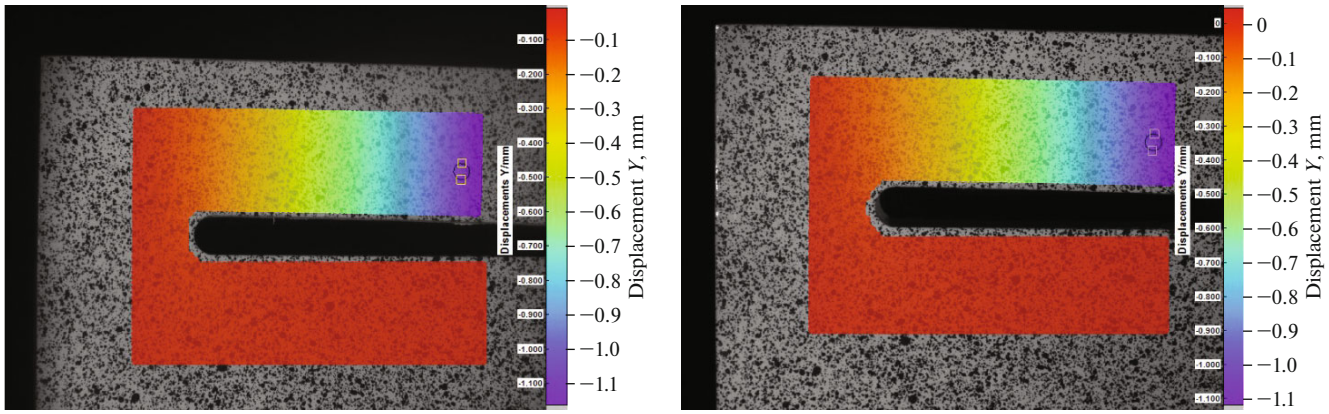

Fig. 7. Measured displacement field in *y* direction by two systems with same loading: left, proposed system, right, standard system.

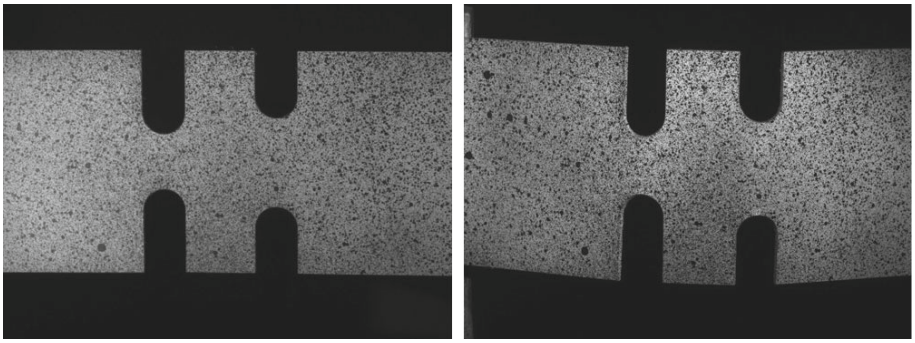

Fig. 8. Images to demostrate the bending test: left, before bending; right, after bending.

The measured strain at the location shown in Fig. 9 from the proposed system and the commercial system is 2.125 and 2.196%, respectively.

4. DISCUSSION AND CONCLUSIONS

In this paper, a single camera 3D-DIC system using a polarized pseudo-stereo system is proposed. The polarization state is adopted to separate the lights from the different views. The proposed system enables two perspective views to be captured in a single camera without reduction of the resolution. Addtionally, the imaging model is the same as the conventional 3D-DIC system, which allows the conventional 3D-DIC algorithm to be directly used by the proposed system. It provides a new path to fulfill the 3D-DIC measurement with a single camera. The drawbacks of the conventional single camera 3D-DIC with a biprism, which include a more than 50% resolution reduction, very limited perspevcive angle, and complex image distortion, have been overcome by the proposed single camera 3D-DIC system. Compared to the other possible solution for the mentioned drawbacks, which uses wavelength to separate the two views, the proposed system does not need multiple lights to illuminate the object, and the loss of light is less than that of the color-camera system.

An industrial camera with a polarizer was used in the experimental validation to simulate the polarization camera. The use of a polarization camera may result in better image quality and system accuracy. However, the experimental validation using the industrial camera with a polarizer still obtained good results. From the tests, the accuracy of the displacement measurement was around 0.01 with a 50 mm lens, and the accuracy of the strain measurement was around 0.1%. The loss of light was around 70% due to the use of the polarizers, while the clear image area is around 90% due to the usage of the reflection system.

Some future study is necessary to optimize the system. The loss of light is still relatively high, due to the use of polarizers in the system, and high power light is necessary for good image quality. In addtion, the reflective-based pseudo-stereo system is more complicated than the refraction-based system. The simplification of the reflection-based system can be further studied, and the possibility of the usage of the refraction-based system can be investigated. Lastly, an integrated system can be studied to make the system more compact and practical.

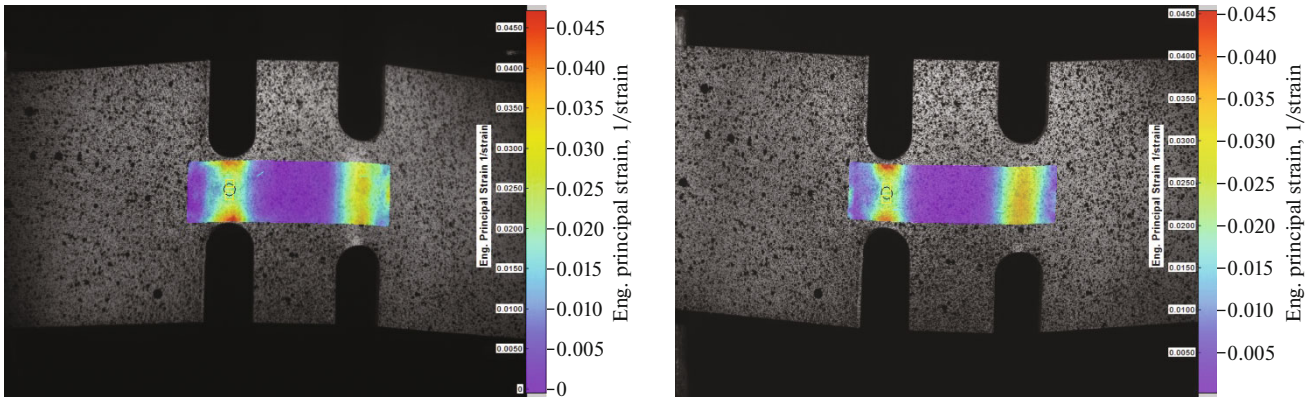

Fig. 9. Strain field with bending: left – proposed system, right – standard system.

ACKNOWLEDGMENTS

The authors would like to express their sincere thanks to Mr. Bernard Sia, who made careful correction of the manuscript as well as the English. The work is partly supported by the Key project of Fujian province science and technology department (2015H6018).

REFERENCES

1. Peters, W.H. and Ranson, W.F., *Optical Eng.*, 1982, vol. 21, no. 3, p. 213427, doi 10.1117/12.7972925
2. Sutton, M.A., Wolters, W.J., Peters, W.H., Ranson, W. F., and McNeill, S.R., *Image Vision Compt.*, 1983, vol. 1, no. 3, p. 133, doi 10.1016/0262-8856(83)90064-1
3. Yamaguchi, I., *J. Phys. E: Sci. Instrum.*, 1986, vol. 19, no. 11, p. 944.
4. Li, J., Xu, W., Xie, X., Siebert, T., and Yang, L., *Int. J. Mater. Res.*, 2016, vol. 107, no 3, p. 245, doi 10.3139/146.111340
5. Sutton, M.A., Yan, J.H., Tiwari, V., Schreier, H.W., and Orteu, J.J., *Optics and Lasers in Eng.*, 2008, vol. 46, no. 10, p. 746, doi 10.1016/j.optlaseng.2008.05. 005
6. Li, J., Xie, X., Yang, G., Zhang, B., Siebert, T., and Yang, L., *Optics and Lasers in Eng.*, 2017, vol. 90, p. 19. doi 10.1016/j.optlaseng.2016.09.012
7. Orteu, J.J., Garric, V., and Devy, M., *Lasers and Optics in Manufact. III,* Int. Soc. for Optics and Photonics, 1997, p. 252.
8. Garcia, D., Orteu, J.J., and Devy, M., *Proc. 2000 Conf. on Vision Modeling and Visualization (VMV-2000)*, Saarbrücken, Germany, 2000, p. 25.
9. Sutton, M.A., Orteu, J.J., and Schreier, H., *Image Correlation for Shape, Motion and Deformation Measurements: Basic Concepts, Theory and Applications,* Springer Science and Business Media, 2009.
10. Ke, X.D., Schreier, H.W., Sutton, M.A., and Wang, Y.Q., *Exper. Mech.*, 2011, vol. 51, no. 4, p. 423, doi 10.1007/s11340-010-9450-3
11. Beberniss, T., Eason, T., and Spottswood, S., *Proc. ISMA2012-USD2012*, 2012, p. 1403.
12. Xie, X., Li, J., Sia, B., Bai, T., Siebert, T., and Yang, L., *J. Strain Anal. Eng. Design*, 2017, vol. 52, no. 1, p. 24, doi 10.1177/0309324716668674
13. Genovese, K., Casaletto, L., Rayas, J. A., Flores, V., and Martinez, A., *Optics and Lasers in Eng.*, 2013, vol. 51, no. 3, p. 278. doi 10.1016/j.optlaseng.2012.10.001
14. Wu, L., Zhu, J., and Xie, H., *Measur. Sci. Technol.*, 2014, vol. 25, no. 11, p. 115008.
15. Pan, B. and Wang, Q., *Optics Express,* 2013, vol. 21, no. 21, p. 25056, doi 10.1364/OE.21.025056
16. Lim, K.B. and Yong, X., *J. Electron. Imaging*, 2005, vol. 14, no. 4, p. 043020.
17. Li, J., Dan, X., Xu, W., Wang, Y., Yang, G. and Yang, L., Optics & Laser Technology, 2017, vol. 95, p. 1. https://doi.org/10.1016/j.optlastec.2017.03.030
18. Wolff, L.B., Mancini, T.A., Pouliquen, P., and Andreou, A.G., *IEEE Trans. Robot. Automat.*, 1997, vol. 13, no. 2, p. 195. doi 10.1109/70.563642
19. Olsen, R.C., Eyler, M., Puetz, A.M., and Esterline, C., *Proc. of SPIE*, 2009, vol. 7461, 74610F-2, doi 10.1117/12.825405
20. http://www.fluxdata.com/imaging-polarimeters
21. Abdel-Aziz, Y.I., *Proc. ASP/UI Symposium on Close-Range Photogrammetry*, Urbana, Illinois, 1971.